ELSEVIER

Surface Science 357–358 (1996) 42–46

surface science

Room temperature deposition of gold onto the diffuse and sharp diffraction spot Si(111)-($\sqrt{3} \times \sqrt{3}$)R30° Au surfaces

Richard Plass *, Laurence D. Marks

Department of Materials Science and Engineering, Northwestern University, Evanston IL 60208, USA

Received 15 August 1995; accepted for publication 4 November 1995

Abstract

Room temperature gold depositions onto Si(111)-($\sqrt{3} \times \sqrt{3}$)R30° Au surfaces with diffuse and sharp diffraction spots [Surf. Sci. 242 (1991) 73] (diffuse and sharp $\sqrt{3} \times \sqrt{3}$ Au hereafter) under UHV conditions has been monitored using transmission electron diffraction (TED). Both systems display an increase in surface structure diffraction spot intensities up to the completion of 1.0 monolayer (ML) after which the surface beams display an exponential decrease in intensity with coverage. The exponential decay rate decreases after roughly 1.33 ML. These results can be attributed to gold initially diffusing to and filling $\sqrt{3} \times \sqrt{3}$ Au gold trimer sites in vacancy type surface domain walls [Surf. Sci. 342 (1995) 233], then filling one of three possible sites on the $\sqrt{3} \times \sqrt{3}$ Au structure with essentially no surface diffusion, disrupting nearby gold trimers. Gold deposition onto the diffuse type structure caused the formation and expansion of satellite arcs around the strongest $\sqrt{3} \times \sqrt{3}$ beams similar to those seen by others [Surf. Sci. 242 (1991) 73; Jpn. J. Appl. Phys. 16 (1977) 891; J. Vac. Sci. Technol. A 10 (1992) 3486] at elevated temperatures while the sharp structure displayed only a modest shoulder formation near the strongest $\sqrt{3} \times \sqrt{3}$ beams.

Keywords: Amorphous surfaces; Computer simulations; Contacts; Electron microscopy; Electron–solid interactions, scattering, diffraction; Epitaxy; Gold; Low index single crystal surfaces; Metal–semiconductor nonmagnetic thin film structures; Physical adsorption; Silicides; Silicon; Surface defects

1. Introduction

Among metal induced surface reconstructions the Si(111)-($\sqrt{3} \times \sqrt{3}$) Au system, which appears at coverages between 0.5 and 1.0 ML after annealing and at higher coverages at elevated temperatures [1,3,4,5], is unique in displaying a rich variety of diffraction features [1,6], small surface domains [7,8], and evidence of two different coverage dependent phases [2,3]. The $\sqrt{3} \times \sqrt{3}$ Au structure has recently been confirmed [2] to consist of sets of gold and silicon trimers together forming a missing top layer twisted trimer structure [9] as shown in Fig. 1. Key features of this structure include the presence of two different domains, the boundary between them can consist either of an expanded silicon double layer leading the diffuse $\sqrt{3} \times \sqrt{3}$ Au structure at lower gold coverages or a gold structure leading to the sharp $\sqrt{3} \times \sqrt{3}$ Au structure at lower gold coverages or a gold structure leading to the sharp $\sqrt{3} \times \sqrt{3}$ Au structure for coverages near 1.0 ML.

However this model alone does not explain all the reported diffraction features. Diffuse diffraction spots, sharp spots, and hexagonal star features, have been reported for surfaces slowly cooled after an-

* Corresponding author. Fax: +1 708 491 7820; e-mail: rplass@merle.acns.nwu.edu.

PII S0039-6028(96)00054-4

nealing while arcs partially surrounding the strongest spots have been seen at elevated temperatures or after rapid cooling [1]. These features are likely related to the relatively small surface domains (only roughly 7 to 8 $\sqrt{3} \times \sqrt{3}$ unit cells across) [7]. Above 1.0 ML Yuhara et al. [4] have noted an incommensurate to commensurate phase transition near 300°C between the Si(111)-(6 × 6) Au surface (believed to be a superstructure of $\sqrt{3} \times \sqrt{3}$ Au [1,6]) and a $\sqrt{3} \times \sqrt{3}$ Au surface with arc features around the strongest beams. In light of our recent results on the $\sqrt{3} \times \sqrt{3}$ Au structure a detailed study of the effects of room temperature gold deposition onto the α and β structures could shed light on the nature of these features. Hasegawa and Ino [10], in studying surface electrical conductivity upon room temperature gold deposition onto these surfaces, have reported only general structure changes.

2. Experimental procedure and analysis

The two $\sqrt{3} \times \sqrt{3}$ Au surfaces were prepared by first mechanically and chemically thinning a Si(111) sample then under UHV conditions cleaning it using cycles of Ar^+ ion milling and electron beam annealing to produce 7 × 7 reconstructed surfaces. Onto the top surface 0.69 or 0.84 ML of gold were deposited and lightly electron beam annealed to form the diffuse and sharp surfaces respectively [8].

The Hitachi UHV-H9000 used in this study has been described elsewhere [11] but for this study a gold evaporator and a quartz crystal were installed directly above the objective lens pole piece. To allow direct kinematical interpretation of the data off-zone crystal tilt conditions were used [12]. In both gold deposition studies the surface structure's TED pattern was recorded on Hi 8 mm video tape. To provide accurate gold coverage in the diffuse $\sqrt{3} \times \sqrt{3}$ Au study the audio signal from the quartz crystal thickness monitor was recorded on one of the video tape's audio tracks. Then to obtain the coverage versus time calibration curve the beat frequencies on the audio track were measured, providing accurate (2%) *relative* coverage measurements. The appearance of various surface structures in the Au on Si(111) system at different coverages was used to determine the absolute coverage. Quantification of the diffraction intensities involved digitizing the tape images (summing one second worth of data) then implementing a cross-correlation technique discussed elsewhere [13] to obtain the final intensities (including a routine for rotational alignment).

3. Results and discussion

A sequence of frames taken from gold deposition on the diffuse $\sqrt{3} \times \sqrt{3}$ Au surface is shown in Fig. 2 with the intensities of the arrowed beams plotted in Fig. 3. First note that up to a total coverage of 1 ML the intensity of the diffuse $\sqrt{3} \times \sqrt{3}$ Au strong beams actually *increases* with increasing gold coverage. This effect is also seen in with gold deposition onto the sharp $\sqrt{3} \times \sqrt{3}$ Au structure though not as pronounced as in the diffuse case. This intensity increase corresponds to newly arrived gold atoms filling gold vacancy type surface domain walls (Fig.

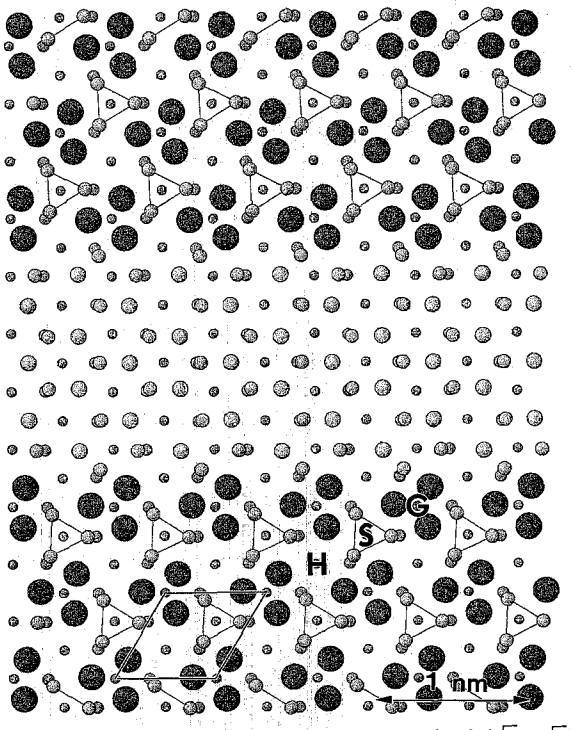

Fig. 1. Schematic of the atomic structure of the Si(111)-($\sqrt{3} \times \sqrt{3}$) Au surface showing its two possible domain configurations above and below a vacancy (with respect to gold) type surface domain wall present in the α-type $\sqrt{3} \times \sqrt{3}$ Au structure (after Plass and Marks [2]).

4) increasing the total number of $\sqrt{3} \times \sqrt{3}$ units contributing to the diffraction intensity. As seen in Fig. 3a, at one monolayer total gold coverage the $\sqrt{3} \times \sqrt{3}$ beams reach their maximum intensities (therefore all beam intensity values have been normalized to these maximum values).

Beyond one total monolayer gold coverage the intensities decay exponentially as shown by the solid curves in Fig 3. The initial decay rate displays a rough correlation to the gold deposition rate: for the diffuse structure the deposition rate was 1.88 ML/min and the decay rate was -2.81 per ML, for the sharp structure the deposition rate was 1.83 ML/min with a -2.69 per ML decay rate. While these differences are near the error levels of the measurements these trends and the first order decay of the intensities show that this system obeys Langmuir kinetics [14] in which, in this case, the decay rate is proportional to the gold deposition rate and inversely proportional to the instantaneous gold coverage. First order kinetics imply a hit and stick decay mechanism with gold surface diffusion playing a minor role in the decay of the surface structure.

A change in the decay rate is evident for both structures at roughly 1.33 monolayers total coverage (arrowed in the solid curves of Fig. 3). That is, for the diffuse structure the initial decay constant is -2.81 ± 0.27 per monolayer between 1.0 and 1.33 ML and -1.93 ± 0.35 per monolayer above 1.33 ML, for the sharp structure the initial decay constant is -2.69 ± 0.05 per monolayer between 1.0 and 1.33 ML and -1.03 ± 0.12 per monolayer above 1.33 ML. The coverage at the change in decay rate, 1.33 ML, corresponds to the filling of one of three possible sites in the $\sqrt{3} \times \sqrt{3}$ Au structure, either the "hollow" site (marked H in Fig. 1), atop the silicon trimer center (S in Fig. 1), or atop the gold trimer center (G in Fig. 1). From the TED data we cannot discern which site is being filled, but we expect the "hollow" site to be the most likely candidate and we are currently in the process of collecting high resolution imaging data to conclusively answer this question.

While not plotted in Fig. 3 for clarity, other weaker surface structure beams farther out in reciprocal space also decay exponentially and more

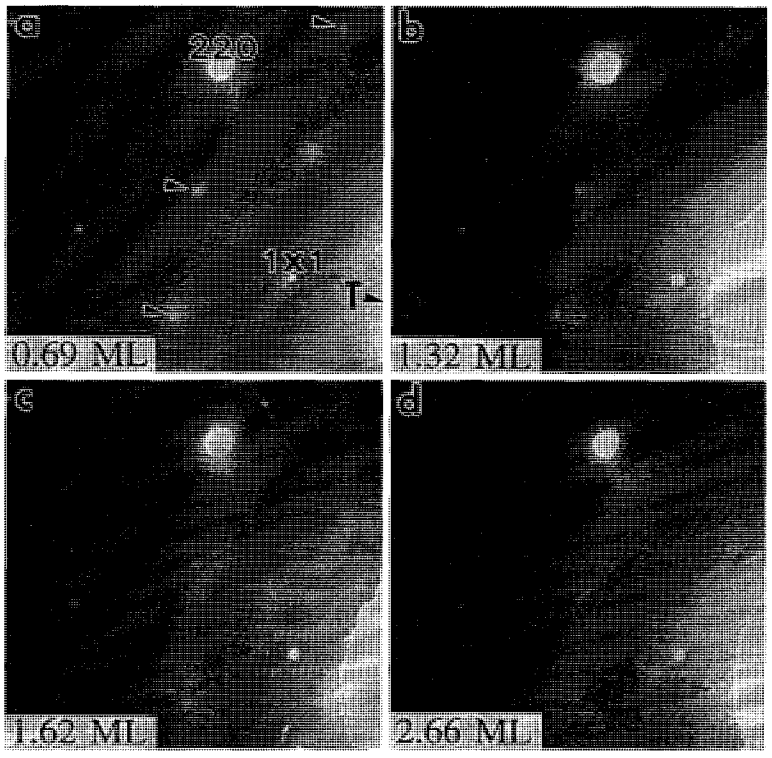

Fig. 2. Diffraction patterns taken from the video taped room temperature gold deposition onto α Si(111)-($\sqrt{3} \times \sqrt{3}$) Au.

quickly than the strongest surface beams. Patterson function analysis of the faster decay of these beams reveals an increasing random static disorder of the atomic sites with increasing gold coverage versus any drastic changes in the $\sqrt{3} \times \sqrt{3}$ Au structure.

Fig. 2 shows the evolution of a broad shoulder (Fig. 2b) to the strongest diffuse $\sqrt{3} \times \sqrt{3}$ Au structure spots followed by the formation of an arc (Fig. 2c) which remains as the beam itself disappears (Fig. 2d). The intensity shoulder does not broaden until after 1.0 ML total gold coverage and if the cross-correlation motif used to determine the beam intensities is modified to include the changing shoulder and arc

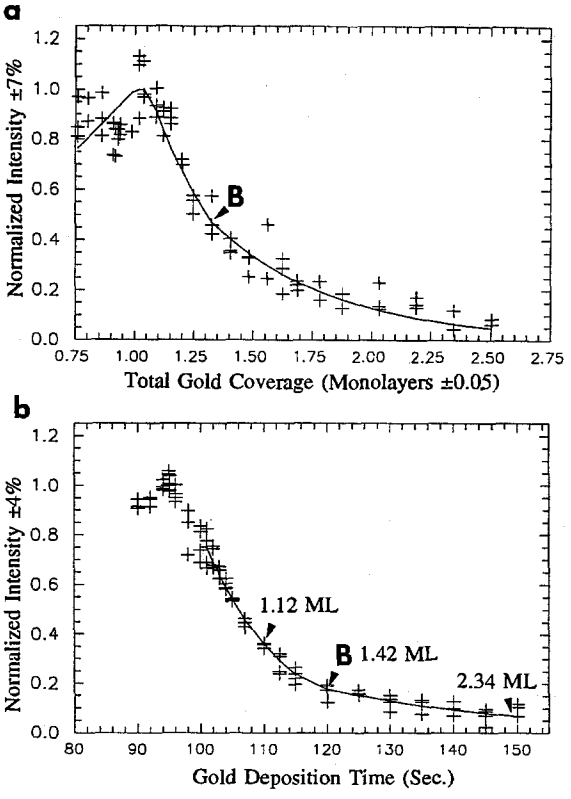

Fig. 3. Plots of the strongest Si(111)-($\sqrt{3} \times \sqrt{3}$) Au diffraction beam intensities (normalized to their maximum values) for (a) the α structure versus total gold coverage and (b) the β structure versus deposition time. The solid curves correspond to first order decay fitting of the data with arrowed break points as discussed in the text. Errors for intensities are conservative estimates based on shot noise statistics. The sharp structure intensities are plotted against time instead of total coverage because the deposition calibration for this sequence was only reliable above 110 s.

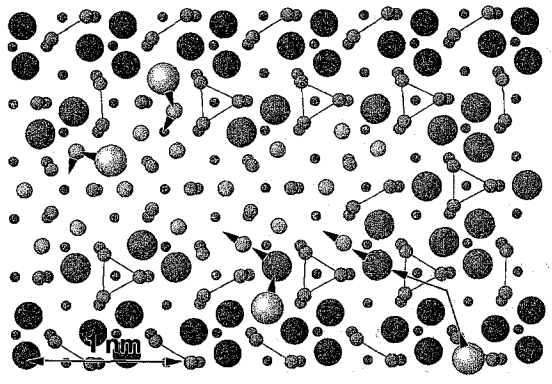

Fig. 4. Schematic atomic structure of a gold vacancy type $\sqrt{3} \times \sqrt{3}$ Au domain wall illustrating how deposited gold atoms can diffuse to and occupy trimer type sites. Just arrived gold atoms are light gray, deposited gold in sites are medium gray and original gold is dark gray.

intensities then the combined spot, shoulder, and arc intensities essentially remain constant with increasing gold coverage. These arcs are very similar to intensity arcs or rings associated with the strong beams at elevated temperatures [1,4,6] but there is one key difference. At elevated temperatures the maximum radius of the arc is about one fourth the distance between the structure beam and the nearest 1×1 type beam, this distance is related to the Si(111)-(6×6) Au unit cell spacing. In our case the maximum arc radius (Fig. 2c) is only two thirds of this value or one sixth the distance between the structure beam and the nearest 1×1 type beam, which allows the arcs to merge with a textured ring forming around the transmitted beam (Fig. 2d). Our results concerning this diffraction ring and its corresponding surface structure will be published separately [15]. In the sharp structure deposition no satellite arc formed and only a moderate shoulder grew from the strongest surface structure beams.

4. Conclusions

We have noted from TED video tape sequences of room temperature gold deposition onto the diffuse and sharp $\sqrt{3} \times \sqrt{3}$ Au surfaces an initial increase in the strongest surface diffraction spot intensities followed by their exponential decay after 1.0 ML total

gold coverage. We attribute the initial rise to gold filling surface domain wall trimer sites and the exponential decay to a hit and stick disordering mechanism. A change in the decay rate at roughly 1.33 ML indicates one of three possible $\sqrt{3} \times \sqrt{3}$ sites is a preferred site for the deposited gold.

Acknowledgement

This work was supported by the Air Force Office of Scientific Research under Grant No. F49620-92-J-0250.

References

[1] S. Takahashi, Y. Tanishiro and K. Takayanagi, Surf. Sci. 242 (1991) 73.
[2] R. Plass and L.D. Marks, Surf. Sci. 342 (1995) 233.
[3] S. Ino, Jpn. J. Appl. Phys. 16 (1977) 891.
[4] J. Yuhara, M. Inoue and K. Morita, J. Vac. Sci. Technol. A 10 (1992) 3486.
[5] G. Lelay and J.P. Faurie, Surf. Sci. 69 (1977) 295.
[6] K. Higashiyama, S. Kono and T. Sagawa, Jpn. J. of Appl. Phys. 25 (1986) L117.
[7] J. Nogami, A.A. Baski and C.F. Quate, Phys. Rev. Lett. 65 (1990) 1611.
[8] T. Takami, D. Fukushi, T. Nakayama, M. Uda and M. Aono, Jpn. J. Appl. Phys. 33 (1994) 3688.
[9] M. Chester and T. Gustafsson, Surf. Sci. 256 (1991) 135.
[10] S. Hasegawa and S. Ino, Surf. Sci. 283 (1993) 438.
[11] L.D. Marks, R. Ai, J.E. Bonevich, M.I. Buckett, D. Dunn, J.P. Zhang, M. Jacoby and P.C. Stair, Ultramicroscopy 37 (1991) 90.
[12] P. Xu and L.D. Marks, Ultramicroscopy 45 (1992) 155.
[13] P. Xu, G. Jayaram and L.D. Marks, Ultramicroscopy 53 (1994) 15.
[14] E.g., A. Zangwill, Physics at Surfaces (Cambridge, New York, 1990) p. 364.
[15] R. Plass and L.D. Marks, Phys. Rev. Lett., submitted.